FEBS Letters 588 (2014) 713–719

FEBS Letters

journal homepage: www.FEBSLetters.org

Effects of palmitoylation on the diffusional movement of BK_{Ca} channels in live cells

Sulgi Kim [a,1], Byoung-Cheol Lee [a,b,c,1], A-Ram Lee [a,b,c], Sehoon Won [a], Chul-Seung Park [a,b,c,*]

[a] School of Life Sciences, Gwangju Institute of Science and Technology (GIST), Gwangju, Republic of Korea
[b] National Leading Research Laboratory, Gwangju Institute of Science and Technology (GIST), Gwangju, Republic of Korea
[c] Cell Dynamics Research Center, Gwangju Institute of Science and Technology (GIST), Gwangju, Republic of Korea

ARTICLE INFO

Article history:
Received 1 September 2013
Revised 21 November 2013
Accepted 8 January 2014
Available online 23 January 2014

Edited by A. Chattopadhyay

Keywords:
BK_{Ca} channel
Palmitoylation
Lateral diffusion
Quantum dot
Single molecule
Lipid raft

ABSTRACT

BK_{Ca} channels are palmitoylated at a cluster of cysteine residues within the cytosolic linker connecting the 1st and 2nd transmembrane domains, and this lipid modification affects their surface expression. To verify the effects of palmitoylation on the diffusional dynamics of BK_{Ca} channels, we investigated their lateral movement. Compared to wild-type channels, the movement of mutant palmitoylation-deficient channels was much less confined and close to random. The diffusion of the mutant channel was also much faster than that of the wild type. Thus, the lateral movement of BK_{Ca} channels is greatly influenced by palmitoylation.

1. Introduction

Large-conductance calcium-activated potassium (BK_{Ca}) channels are a member of the *Slo* family of potassium-selective ion channels, which have large single-channel conductance and are dually activated by membrane depolarization and an increase in intracellular calcium concentration [1–3]. BK_{Ca} channels are composed of a pore-forming α-subunit and a modulatory β-subunit. BK_{Ca} channels are widely expressed in both neuronal and non-neuronal tissues, and play important roles in various physiological processes such as neuronal excitability, action potential firing, neurotransmitter release and smooth-muscle contraction [4].

Protein *S*-palmitoylation (or palmitoylation) is a classic and common lipid modification, which involves the covalent attachment of 16-carbon palmitate to an intracellular cysteine (Cys) residue. Many proteins, including voltage- and ligand-gated ion channels, are palmitoylated [5,6]. Palmitoylation is known to control the functioning of ion channels at multiple stages of their life cycle, from maturation to trafficking and regulation of the mature channel [7].

The α-subunits of the BK_{Ca} channel are palmitoylated in at least two different regions. An evolutionarily conserved Cys residue is palmitoylated at an alternatively spliced insert, called the stress-regulated exon (STREX), in the cytosolic C-terminus [8]. The channel α-subunit is also palmitoylated at a cluster of three Cys residues within the cytosolic linker connecting the 1st and 2nd transmembrane domains (S0–S1 linker) [9]. Recently, it was also reported that the β4-subunit of BK_{Ca} channels could be palmitoylated at a cysteine residue (C193) in the intracellular C-terminus [10].

In our previous studies, we investigated the movements of individual BK_{Ca} channels in live cells using quantum dots [11,12]. We demonstrated that BK_{Ca} channels diffuse within highly confined membrane areas [11]. We also reported that the lateral movement of BK_{Ca} channels can be restricted by cytoskeletal components via an actin-binding motif at the cytosolic C-terminus [12]. Actin depolymerization led to a significant increase in the area of confinement, as did a point mutation in the actin-binding motif; however, the lateral diffusion of the channel remained confined.

Motivated by these previous results, we focused our attention in this study on the effects of palmitoylation on the membrane diffusion of BK_{Ca} channels. By monitoring and analyzing the movement of QD-based single particles of the wild-type and a mutant

* Corresponding author at: School of Life Sciences, Gwangju Institute of Science and Technology (GIST), 123 Cheomdangwagi-ro, Buk-gu, Gwangju 500-712, Republic of Korea. Fax: +82 62 970 2484.
E-mail address: cspark@gist.ac.kr (C.-S. Park).
[1] These authors contributed equally to this work.

0014-5793/$36.00
http://dx.doi.org/10.1016/j.febslet.2014.01.014

channel in which three Cys residues in the S0–S1 linker region were substituted with alanine (Ala), we were able to show that palmitoylation is critical for the confined diffusion of BK_{Ca} channels within the cell surface membrane.

2. Materials and methods

2.1. Cell culture and expression of BK_{Ca} channels

The α subunit of the rat BK_{Ca} channel, rSlo (GenBank accession number AF135265), was tagged at its N-terminus with the acceptor peptide for biotin labeling [13]. For generation of the palmitoylation-deficient channel (C53:54:56A), site-directed mutagenesis was performed using the QuickChange site-directed mutagenesis kit (Stratagene, Santa Clara, CA). The modified DNAs were subcloned into pcDNA3.1 (+) vector (Invitrogen, Carlsbad, CA). COS-7 cells were maintained in DMEM (Thermo, Waltham, MA) supplemented with 10% fetal bovine serum (Thermo) and 1% antibiotic (Gibco-RRL, Carlsbad, CA) in 5% CO_2 at 37 °C. COS-7 cells were plated onto 18 mm coverslips (Marienfeld, Lauda-Königshofen, Germany) coated with 0.05 mg/ml poly-D-lysine (Sigma–Aldrich, St. Louis, MO) at a density of 1.5×10^4 cells per coverslip. For transient expression, the plasmid harboring rSlo cDNA was cotransfected into COS-7 cells with another plasmid, pDisplay BirA-ER, in a 3:1 ratio using Lipofectamine™ 2000 (Invitrogen).

2.2. Quantum dot labeling and live cell imaging

Forty-eight hours after transfection, cells on coverslips were washed carefully with Tyrode solution and were incubated with 0.5 nM streptavidin-conjugated QD605 (Invitrogen) for 10 min at room temperature [11,12]. Cells were observed with a microscope (Olympus IX-81, Olympus, Tokyo, Japan) connected to a charge-coupled device (CCD) camera (Andor, Belfast, Northern Island). The excitation and emission of quantum dots were controlled by specific QD605 filters (SemRock Corp., Rochester, NY). Images were captured using the commercial software MetaMorph (Universal Imaging, Downingtown, PA). Images were collected at 100 ms time intervals over 30 s using the stream-recording mode at room temperature. To deplete cholesterol from lipid raft domains, cells in Tyrode solution were treated for 30 min at 37 °C with methyl-β-cyclodextrin (Sigma–Aldrich, 10 mM). Then, COS-7 cells were incubated with 0.5 nM streptavidin-conjugated QD605 in Tyrode for 10 min at room temperature [11,12].

2.3. Analysis of channel movements

All images were analyzed using the commercial software, MetaMorph. Changes in the *X–Y* coordinates of dots were tracked over time using imaging software. Mean square displacement (MSD) values were obtained over 300 sequential frames (or every 100 ms) and plotted against time as described in previous studies [11,12]. The instantaneous diffusion coefficient (D_{init}) was calculated by fitting the slope of each MSD curve in every 1.0 s interval of the total 30 s plot.

2.4. Electrophysiological recording

All macroscopic current recordings were performed using the patch-clamp method in an inside-out configuration [11,12]. Patch pipettes were fabricated from borosilicate glass (WPI, Sarasota, FL) and then fire-polished (3–5 MΩ). The channel currents were amplified using an Axopatch 200B (Axon Instruments, Foster City, CA), low-pass filtered at 1 kHz using a four-pole Bessel filter, and digitized using a Digidata 1200A (Axon Instruments). The symmetric recording solutions contained the following components: 116 mM KOH, 4 mM KCl, 10 mM HEPES, and 5 mM EGTA. The pH was adjusted to 7.2 with 2-[Nmorpholino] ethanesulfonic acid (MES). For the acquisition and analysis of macroscopic recording data, commercial software packages, Clampex 8.0 (Axon Instruments) and Origin 6.0 (OriginLab Corp., Northampton, MA), were used.

2.5. Isolation of detergent-resistant membranes

Cells were lysed on ice in 250 μl of 1% Triton in MNE-buffer [25 mM MES (pH 6.5), 150 mM NaCl, 5 mM EDTA], dounced ten times using a dounce glass homogenizer, and mixed with 250 μl of 80% sucrose made with MNE-buffer. After being transferred to a centrifuge tube, the lysate was overlaid with 400 μl of 30% sucrose in MNE-buffer, followed by 200 μl of 5% sucrose in MNE. After centrifugation for 5 h at 200000×*g* in a Beckman OptimaTM TL Ultracentrifuge (Beckman Coulter, Brea, CA), 80 μl gradient fractions were collected from the top of the gradient. Flotillin-1 antibody was used as a lipid raft marker.

3. Results

3.1. Expression and characterization of wild-type and palmitoylation-deficient BK_{Ca} channels

Since lipid modification can affect the dynamics of membrane proteins, we decided to investigate the functional effects of palmitoylation on the lateral diffusion of BK_{Ca} channels. BK_{Ca} channels lacking the STREX insert are palmitoylated only at the cytosolic S0–S1 linker [9]. As reported previously for the mouse BK_{Ca} channel [9], a cluster of three Cys residues (Cys53, Cys54, and Cys56) is also conserved in the S0–S1 linker of the rat BK_{Ca} channel; these residues are highly likely to be palmitoylated according to the predictions of CSS-Palm 3.0 software (http://csspalm.biocuckoo.org/).

To specifically label BK_{Ca} channels using QDs in live cells, we utilized a modified version of the α subunit of the rat BK_{Ca} channel (rSlo) [12]. The N-terminus of rSlo was tagged with an amino-acid sequence called acceptor peptide (AP) (Fig. 1A); the lysine residue in AP can then be biotinylated by *Escherichia coli* biotin ligase targeted to the lumen of the endoplasmic reticulum, BirA-ER, and the channel is subsequently expressed on the cell surface [13]. The N-terminal biotins are exposed to the extracellular side of the plasma membrane and can be labeled by streptavidin-conjugated QDs. In addition to the AP-tagged wild-type channel, a palmitoylation-deficient mutant channel (C53:54:56A) was constructed in which the three Cys residues in the S0–S1 linker were substituted with Ala residues (Fig. 1A, *red*).

Before monitoring the movement of mutant channels, we assessed the cell surface expression of C53:54:56A, since this was significantly reduced by the triple Cys mutation at the linker in mouse BK_{Ca} channels [9]. We noticed that the expression of C53:54:56A channel in total lysate was decreased by about 20% compared to the WT channel (Fig. 1B). Consistent with the previous report [9], surface expression of the palmitoylation-deficient mutant channel in COS-7 cells was also significantly reduced by approximately 2-fold (Fig. 1B). COS-7 cells expressing the WT and a C53:54:56A were labeled robustly with QDs (Fig. 1C).

3.2. Electrophysiological characterization of wild-type and palmitoylation-deficient BK_{Ca} channels

The functional expression of the mutant channel was also corroborated by electrophysiological recording. We measured the ionic currents evoked by wild-type and mutant channels expressed

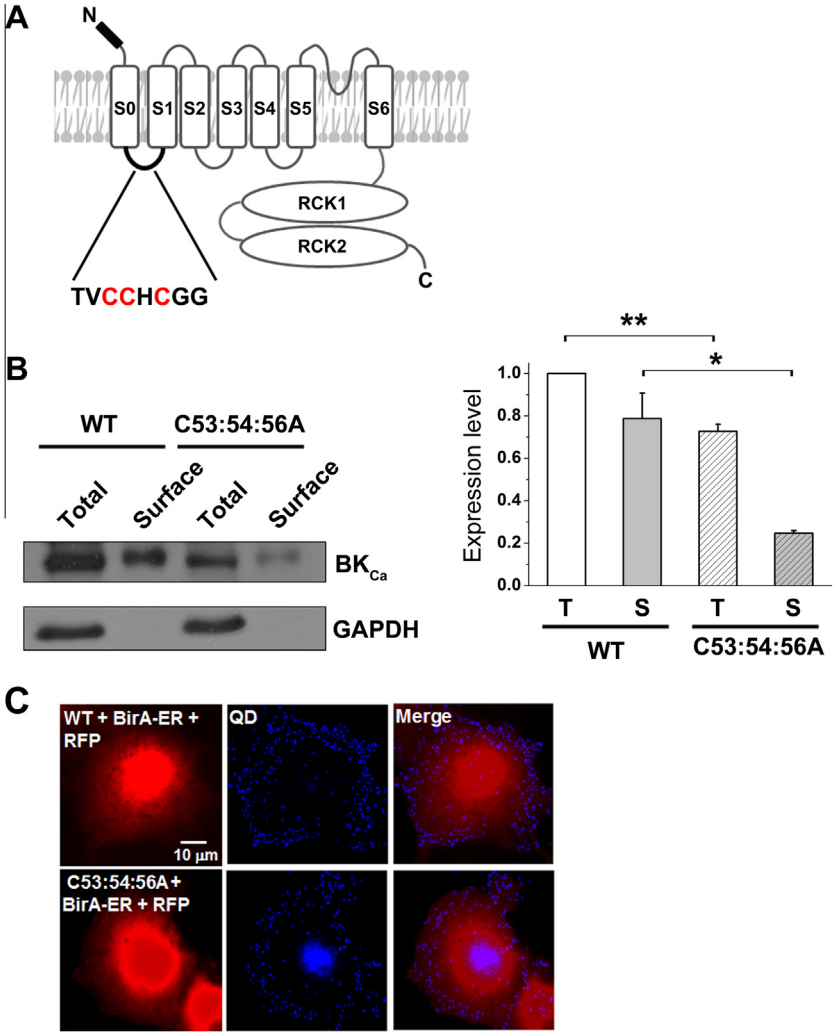

Fig. 1. Surface expression of QD-labeled WT and palmitoylation-deficient BK_{Ca} channels in COS-7 cells. (A) Schematic illustration of the rat BK_{Ca} channel α subunit (rSlo) used in this experiment. The N-terminal AP-tag is depicted with a *black* box. Cysteine residues predicted to be palmitoylated in the S0–S1 linker of the cytosolic domain, are indicated in *red*. (B) Cell surface biotinylation of WT and C53:54:56A channels. Cells transfected with the WT and C53:54:56A were biotinylated and subsequently precipitated. The precipitates were subjected to immunoblot analysis (*left*). Densitometric quantitation of the total (*T*) and surface (*S*) expression of the two channel types was conducted (*right*). $^{*}P < 0.05$ and $^{**}P < 0.01$ by paired Student's *t*-test. (C) Representative images of cells expressing QD-labeled WT and C53:54:56A channels. Cells expressing WT, C53:54:56A and RFP (Red fluorescent protein) are shown in *red* (*left* column). Fluorescence from RFP is not conjugated to the channel protein. QD605 is shown in *blue* (*center* column). Merged images are also shown (*right* column).

in COS-7 cells. The channels were activated by a series of voltage pulses ranging from −80 mV to 200 mV, in 10 mV increments at 3 μM $[Ca^{2+}]_i$. As seen in the biotinylation assay, the overall electrophysiological activity of the mutant channel was lower than that of WT channels (Fig. 2A). The *G–V* relationships and $V_{1/2}$ values of the mutant channel at different Ca^{2+} concentrations were not significantly different from those of the WT BK_{Ca} channel (Fig. 2B and C). These results are consistent with a previous report in which no significant functional effects were observed in the mouse BK_{Ca} channel following mutations at the equivalent sites [9].

3.3. Effects of palmitoylation on the membrane movements of BK_{Ca} channels

We then investigated the effects of palmitoylation on the membrane dynamics of QD-labeled BK_{Ca} channels in live COS-7 cells using time-lapse imaging. Individual fluorescent images were tracked at 100 ms time intervals over 30 s (Supplement Movie 1–2). The trajectories of four different QD-labeled WT and mutant BK_{Ca} channels are shown at 0, 10, 20, and 30 s (Fig. 3A). As described in our previous report [11], the overall movement of the QD-labeled WT channels is highly confined. When compared with the WT, C53:54:56A appeared to be less confined and some QD-labeled mutant channels migrated over much wider areas in the COS-7 cell membrane (Fig. 3A, *arrowhead*).

We then analyzed the movement of WT and mutant channels quantitatively using two different criteria: the MSD versus time plot, and the population histogram of MSD over 30 s (Fig. 3B and C). The QD-labeled WT channels showed highly confined movement in the time vs. MSD plot. The initial diffusion coefficient, D_{init}, and the confinement area for diffusion were estimated as 0.015 $\mu m^2/s$ and 1.45 μm^2, respectively, for the WT channel (Fig. 3B). The histogram of MSD values at 30 s showed that the WT channels were a homogenous population (Fig. 3C). Quantitative analyses revealed significant differences in the movement of the C53:54:56A channels (Fig. 3B and C). The MSD vs. time curve of the C53:54:56A channel was significantly linearized compared to that of the WT channel, with only a slight curvature. The D_{init} and the confinement area were estimated as 0.024 $\mu m^2/s$ and 3.09 μm^2 for C53:54:56A, respectively, indicating that the removal

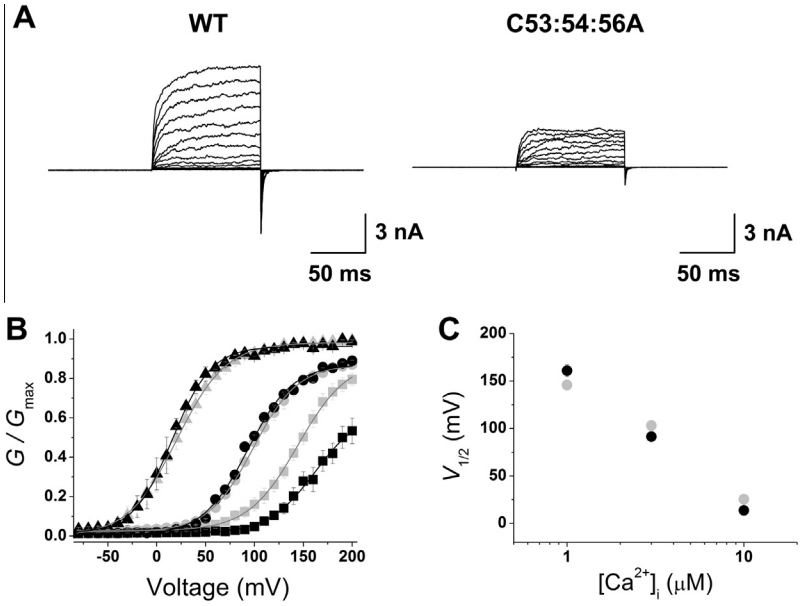

Fig. 2. Electrophysiological characterization of QD-labeled WT and palmitoylation-deficient BK_{Ca} channels in COS-7 cells. (A) Representative current traces from WT (*left*) and C53:54:56A channels (*right*) are shown. Ionic currents were evoked with 100 ms voltage steps from −80 mV to 150 mV. (B and C) Normalized *G–V* relationships (B) and half-activation voltage ($V_{1/2}$) (C) of the BK_{Ca} channel for various concentrations of Ca^{2+} (*black*, WT; *grey*, C53:54:56A). The symbols represent different concentrations of Ca^{2+}: 1 (■), 3 (●), 10 μM (▲). Each data point represents the mean value ± the S.E.M.

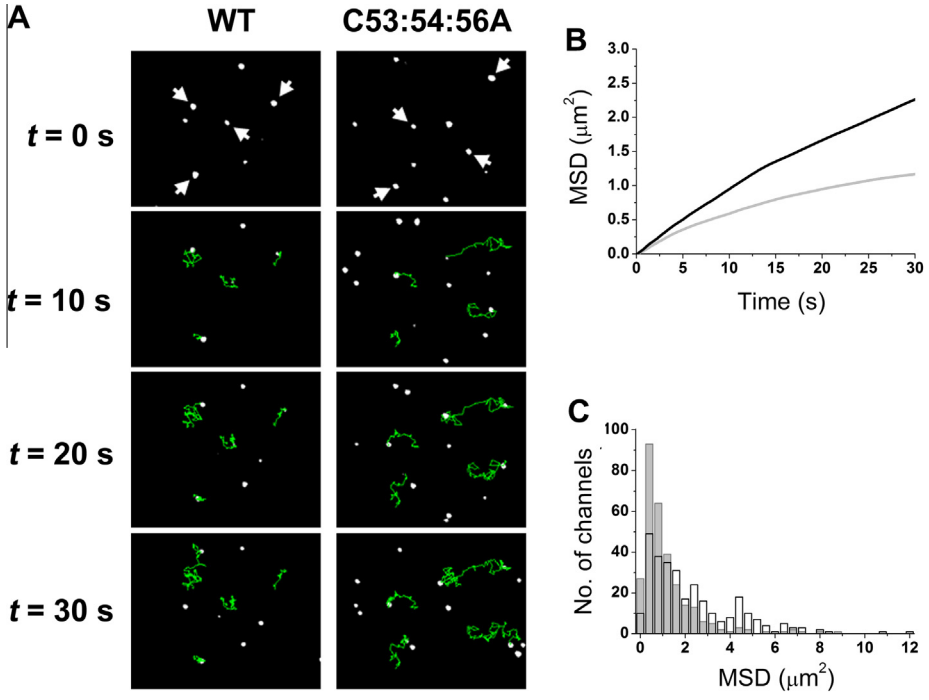

Fig. 3. Effects of mutations at palmitoylation sites in the S0–S1 linker region on membrane motility in COS-7 cells. (A) Trajectories of QD-labeled WT and C53:54:56A channels in COS-7 cells. Fluorescence images of COS-7 cells transfected with WT (*left* column) or C53:54:56A (*right* column) are shown at different time-points (0, 10, 20, and 30 s). Time-lapse trajectories of four different dots (*arrow*) are superimposed (*green*). (B) Time-dependent MSD plot of WT and C53:54:56A. Time-dependent changes in average MSD are shown for WT (*grey* line) and C53:54:56A (*black* line). (C) MSD histogram of QD-labeled WT and C53:54:56A. The distribution of MSD at 30 s is shown for WT (*grey* bars, $n = 300$) and C53:54:56A (*open* bars, $n = 300$) channels.

of palmitoyl groups enables the channels to diffuse 60% more rapidly over a 2.1-fold larger area. It was also evident from the MSD histogram that the pattern of diffusion had become much more heterogeneous in the case of the C53:54:56A channel. The fraction of the channel population with MSD values greater than 2 μm^2 was increased from 17.7% to 45.7% by the mutation, suggesting that a significant proportion of BK_{Ca} channels lacking palmitoyl groups can cover larger areas by diffusion.

Next, we compared the migration distance of individual channels in a single imaging-time. Over 120 000 dots were selected and their migration distances calculated every 100 ms for 30 s. When we plotted the migration distances of WT and C53:54:56A

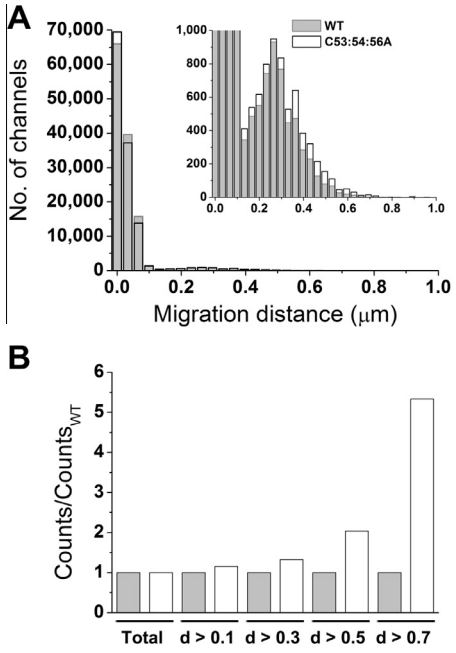

Fig. 4. Effects of palmitoylation of BK_{Ca} channels on migration length. (A) Histogram of migration distance of QD-labeled WT and C53:54:56A channels. Calculated migration length at a time (for 100 ms) of WT (*grey* bars) and C53:54:56A channels (*open* bars) are shown (inset, magnified view; $n = 120000$ each). (B) Normalized counts of migration distance in 100 ms time periods for WT and C53:54:56A channels (*d*, migration distance). Migrations were categorized according to their length and the ratio of C53:54:56A: WT migration events calculated within each subgroup.

channels, both channel types exhibited two clearly distinct migration patterns: major migrations shorter than 0.1 μm and minor migrations peaking at 0.264 μm. Although the overall migration patterns were similar (Fig. 4A), there were clear quantitative differences between WT and C53:54:56A channels. By magnifying the *y*-axis of the plot (Fig. 4A, *inset*), we found that the number of channels experiencing a longer migration (>0.1 μm) was significantly increased, from a total of 5609 WT channels to 6683 mutant channels. When we divided the migration distance into subcategories, we saw that the proportion of the channel population traveling much longer distances was dramatically increased in the palmitoylation-deficient mutants (Fig. 4B). In addition, the mean distances covered by WT and C53:54:56A channels during each migration event were 0.266 ± 0.001 μm and 0.284 ± 0.001 μm, respectively, indicating that some of the mutant channels can diffuse much more rapidly than WT channels. However, only small fraction of BK_{Ca} channels seemed to be affected by the loss of palmitoylation.

3.4. Confinement of BK_{Ca} channels by disruption of lipid rafts

Since a specific BK_{Ca} channel variant was shown to be localized to the lipid rafts of glioma cells [14], we examined whether the membrane dynamics of BK_{Ca} channels expressed in COS-7 cells are influenced by these lipid microdomains. To disrupt the lipid rafts pharmacologically, we treated COS-7 cells expressing the WT or C53:54:56A channels with 10 mM methyl-β-cyclodextrin (MβCD). Then, we tracked individual QD-labeled BK_{Ca} channels at 100 ms time intervals over 30 s. Movements of the QD-labeled WT and C53:54:56A channels were dramatically altered by treatment with MβCD (Fig. 5A). Treatment of 2% DMSO (control) did not affect the movements of WT and C53:54:56A channels significantly. Contrary to our expectations, movements of WT and C53:54:56A were markedly restricted by the depletion of cholesterol. MSD vs. time plots showed that both WT and the mutant channel became almost immobile following treatment with MβCD (Fig. 5B).

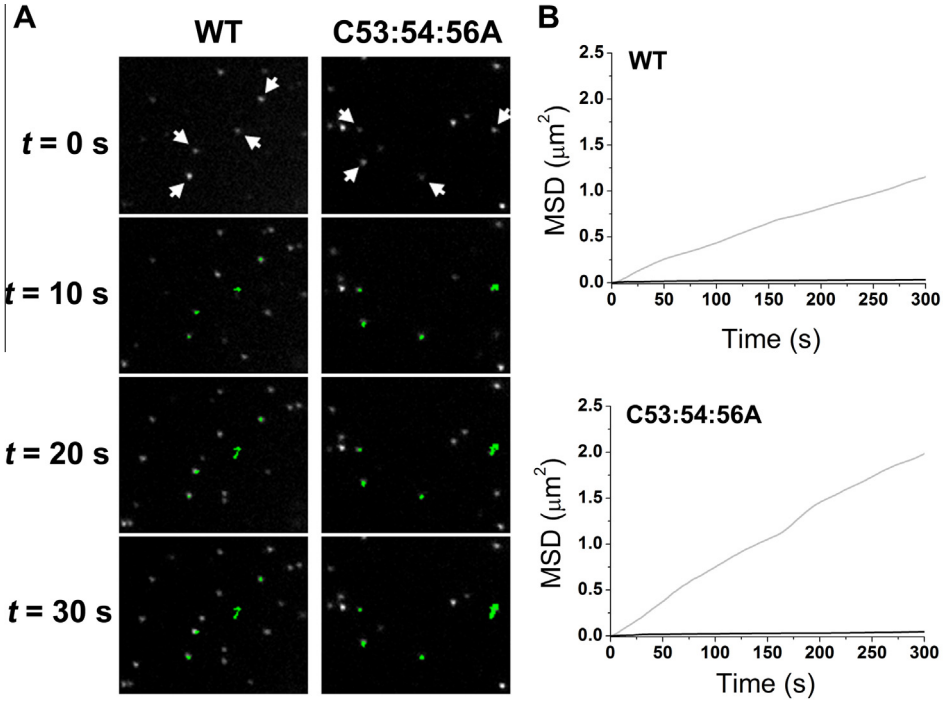

Fig. 5. Effect of disruption of lipid rafts on the movement of QD-labeled BK_{Ca} channels in COS-7 cells. (A) Trajectories of QD-labeled WT (*left* column) and C53:54:56A (*right* column) channels after application of methyl-β-cyclodextrin (MβCD). COS-7 cells expressing WT and C53:54:56A channels were treated with 10 mM MβCD for 30 min. Fluorescence images of COS-7 cells transfected with WT and C53:54:56A channels are shown at different time-points (0, 10, 20, and 30 s). Time-lapse trajectories of four different dots (*arrow*) are superimposed (*green*). (B) Time-dependent MSD plot and effects of MβCD. The time-dependent changes in average MSD of WT (*upper*) and C53:54:56A (*lower*) channels are shown before (*grey* line) and after treatment with MβCD (*black* line).

4. Discussion

In our previous study, we found that the movement of BK_{Ca} channels is highly confined in COS-7 cells [11]. To reveal the molecular mechanism behind this confinement, we investigated the roles of cytoskeletal components in BK_{Ca} channel diffusion by disrupting the cytoskeleton and mutagenizing an actin-binding motif [12]. We showed that disruption of filamentous actin markedly increased the mobility of BK_{Ca} channels, as did a single mutation in the actin-binding motif. Although the area of confinement was significantly increased by actin depolarization, membrane diffusion still remained confined [12]. Since lipid microdomains have been suggested to be one potential factor constraining the lateral diffusion of membrane proteins [15,16], we examined the effects of palmitoylation on membrane dynamics of BK_{Ca} channels in this study.

By analyzing the diffusional movements of wild-type and palmitoylation-deficient channels at the level of single molecules, we were able to reveal the effects of palmitoylation on the membrane diffusion of BK_{Ca} channels. First, the overall movement of the channels was significantly randomized by the mutation as indicated by a near-linear MSD vs. time plot (Fig. 3B). This effect was also manifested in the 2.1-fold increase in the confinement area of palmitoylation-deficient channels estimated from the asymptote of the plot. Second, the channels lacking palmitates moved more rapidly than wild-type channels, as indicated by a 60% increase in the initial diffusion coefficient. Detailed analyses of individual channel movements revealed intriguing but rather perplexing effects of palmitoylation. In terms of their diffusional behaviors, the palmitoylation-deficient channels were much more heterogeneous than the wild-type channels. It was evident that a significant number of mutant channels diffuse more rapidly within larger areas (Fig. 3C). Moreover, a considerable number of channels were recruited from the major static population to more mobile populations (Fig. 4A). It remains to be determined why only a small proportion of the channels were affected by the de-palmitoylation and what it is that makes mutant channels lacking palmitates diffuse more rapidly in a near random fashion. One possibility is that the micro-environment of the cell membrane plays a role since the lipid microdomain influences the movement of membrane proteins [17]. Protein palmitoylation was found to promote the localization of membrane proteins to lipid rafts [18,19].

However, we were able to rule out the involvement of lipid rafts as a potential explanation for why de-palmitoylation releases BK_{Ca} channels from confined diffusion. As shown in Fig. 5, depletion of cholesterol and thus disruption of lipid rafts led to the movement of BK_{Ca} channels in COS-7 cells becoming drastically more confined. Although this was not anticipated for BK_{Ca} channels, several other membrane proteins are known to exhibit such behavior; for example, the diffusion of aquaporin 1 was impeded by depletion of cholesterol with methyl-β-cyclodextrin [20]. In fact, the movement of membrane proteins could be obstructed by solid-like lipid or protein clusters created by cholesterol depletion [21].

We reported previously that the diffusional movement of BK_{Ca} channels can be restricted by actin cytoskeleton via an actin-binding motif at its cytosolic C-terminus [12]. However, the effects of palmitoylation on channel diffusion found in the present study appear to be independent of actin cytoskeleton. When we monitored the movement of doubly-mutated channels (L1048A/C53:54:56A) in which both the actin-binding motif (L1048) and the palmitoylation sites (C53:54:56) were simultaneously mutated, L1048A/C53:54:56A channels did not show any additional or synergistic effects compared to C53:54:56A channels (Supplement Fig. 1).

To reinforce the imaging results, we also performed biochemical experiments in which we used sucrose gradient centrifugation to isolate the buoyant lipid raft fractions from COS-7 cells expressing both wild-type and mutant channels (Supplement Fig. 2). The results showed few differences in the expression of WT and C53:54:56A channels in 12 fractions, especially in the lipid raft domain. These results further strengthen the notion that the increased diffusion of the de-palmitoylated mutant channels is not due to the release of BK_{Ca} channels from lipid raft domains. Instead, the reduced confinement of palmitoylation-deficient channels might be the result of the loss of palmitoylation-dependent signaling or the alteration of protein structures.

In conclusion, we have demonstrated that the movement of BK_{Ca} channels can be affected by lipid modification of the channel in live COS-7 cells. Palmitoylation at the S0–S1 linker of the BK_{Ca} channel may play a critical role in restricting the lateral diffusion of the channel.

Acknowledgments

This work was supported by Grants for the National Leading Research Laboratories [2011-0028665] and the Science Research Center of Excellence Program [2007-0056157] of Korea Ministry of Science, ICT& Future Planning (MSIP)/National Research Foundation of Korea (NRF).

Appendix A. Supplementary data

Supplementary data associated with this article can be found, in the online version, at http://dx.doi.org/10.1016/j.febslet.2014.01.014.

References

[1] Pallotta, B.S., Magleby, K.L. and Barrett, J.N. (1981) Single channel recordings of Ca2+-activated K+ currents in rat muscle cell culture. Nature 293, 471–474.
[2] Cui, J., Cox, D.H. and Aldrich, R.W. (1997) Intrinsic voltage dependence and Ca2+ regulation of mslo large conductance Ca-activated K+ channels. J. Gen. Physiol. 109, 647–673.
[3] Zhang, X., Solaro, C.R. and Lingle, C.J. (2001) Allosteric regulation of BK channel gating by Ca(2+) and Mg(2+) through a nonselective, low affinity divalent cation site. J. Gen. Physiol. 118, 607–636.
[4] Berkefeld, H., Fakler, B. and Schulte, U. (2010) Ca2+-activated K+ channels: from protein complexes to function. Physiol. Rev. 90, 1437–1459.
[5] Schmidt, J.W. and Catterall, W.A. (1987) Palmitylation, sulfation, and glycosylation of the alpha subunit of the sodium channel. Role of post-translational modifications in channel assembly. J. Biol. Chem. 262, 13713–13723.
[6] Pickering, D.S., Taverna, F.A., Salter, M.W. and Hampson, D.R. (1995) Palmitoylation of the GluR6 kainate receptor. Proc. Natl. Acad. Sci. U.S.A. 92, 12090–12094.
[7] Shipston, M.J. Ion channel regulation by protein palmitoylation. J. Biol. Chem. 286, 2011, 8709–8716.
[8] Tian, L., Jeffries, O., McClafferty, H., Molyvdas, A., Rowe, I.C., Saleem, F., Chen, L., Greaves, J., Chamberlain, L.H., Knaus, H.G., Ruth, P. and Shipston, M.J. (2008) Palmitoylation gates phosphorylation-dependent regulation of BK potassium channels. Proc. Natl. Acad. Sci. U.S.A. 105, 21006–21011.
[9] Jeffries, O., Geiger, N., Rowe, I.C., Tian, L., McClafferty, H., Chen, L., Bi, D., Knaus, H.G., Ruth, P. and Shipston, M.J. (2010) Palmitoylation of the S0–S1 linker regulates cell surface expression of voltage- and calcium-activated potassium (BK) channels. J. Biol. Chem. 285, 33307–33314.
[10] Chen, L., Bi, D., Tian, L., McClafferty, H., Steeb, F., Ruth, P., Knaus, H.G. and Shipston, M.J. (2013) Palmitoylation of the beta4-subunit regulates surface expression of large conductance calcium-activated potassium channel splice variants. J. Biol. Chem. 288, 13136–13144.
[11] Won, S., Kim, H.D., Kim, J.Y., Lee, B.C., Chang, S. and Park, C.S. (2010) Movements of individual BKCa channels in live cell membrane monitored by site-specific labeling using quantum dots. Biophys. J. 99, 2853–2862.
[12] Won, S., Lee, B.C. and Park, C.S. (2011) Functional effects of cytoskeletal components on the lateral movement of individual BKCa channels expressed in live COS-7 cell membrane. FEBS Lett. 585, 2323–2330.
[13] Howarth, M. and Ting, A.Y. (2008) Imaging proteins in live mammalian cells with biotin ligase and monovalent streptavidin. Nat. Protoc. 3, 534–545.
[14] Weaver, A.K., Olsen, M.L., McFerrin, M.B. and Sontheimer, H. (2007) BK channels are linked to inositol 1,4,5-triphosphate receptors via lipid rafts: a novel mechanism for coupling [Ca(2+)](i) to ion channel activation. J. Biol. Chem. 282, 31558–31568.

[15] Sheets, E.D., Lee, G.M., Simson, R. and Jacobson, K. (1997) Transient confinement of a glycosylphosphatidylinositol-anchored protein in the plasma membrane. Biochemistry 36, 12449–12458.
[16] Jacobson, K. and Dietrich, C. (1999) Looking at lipid rafts? Trends Cell Biol. 9, 87–91.
[17] Dietrich, C., Yang, B., Fujiwara, T., Kusumi, A. and Jacobson, K. (2002) Relationship of lipid rafts to transient confinement zones detected by single particle tracking. Biophys. J. 82, 274–284.
[18] Crise, B. and Rose, J.K. (1992) Identification of palmitoylation sites on CD4, the human immunodeficiency virus receptor. J. Biol. Chem. 267, 13593–13597.
[19] Zhang, W., Trible, R.P. and Samelson, L.E. (1998) LAT palmitoylation: its essential role in membrane microdomain targeting and tyrosine phosphorylation during T cell activation. Immunity 9, 239–246.
[20] Crane, J.M. and Verkman, A.S. (2008) Long-range nonanomalous diffusion of quantum dot-labeled aquaporin-1 water channels in the cell plasma membrane. Biophys. J. 94, 702–713.
[21] Nishimura, S.Y., Vrljic, M., Klein, L.O., McConnell, H.M. and Moerner, W.E. (2006) Cholesterol depletion induces solid-like regions in the plasma membrane. Biophys. J. 90, 927–938.